

# Surface relief grating recording in amorphous chalcogenide and azobenzene compounds

J. TETERIS\*

*Institute of Solid State Physics, University of Latvia, 8 Kengaraga Str., LV-1063, Riga, Latvia*

The direct formation of surface relief gratings (SRG) in amorphous chalcogenide and low molecular weight azo-benzene containing organic glass films during holographic recording was studied. It has been shown that the course of SRG growth curves can be divided in three development stages: an induction period of photo-induced birefringence, linear growing of SRGs and saturation of SRG inscription process. The influence of the photo-induced birefringence on the relief formation process in amorphous As-S and As-S-Se films was evaluated and compared with the measurements on azo-benzene containing organic glass films. It was shown that the saturation of SRG formation depends on the surface tension of recording material.

(Received February 5, 2018, accepted June 7, 2018)

*Keywords:* Surface relief gratings, Holographic recording, Amorphous chalcogenide films, Azo-dye polymers

## 1. Introduction

The properties and the application of “soft materials” including organic and inorganic polymers are based on weak but nevertheless long-range interactions among the molecular constituents [1]. These interactions lead to the formation of static and frequently also dynamic structures and changes of physical and chemical properties that can be changed by light. Photo-induced structural changes in soft materials play the key role in advanced technologies: chalcogenide thin films are used as storage media of information; organic and inorganic photoresists and related materials necessary to produce advanced electronics hardware [2]. Photo-induced alignment of molecules in azo-containing polymers causes an optical birefringence – the basic condition for polarization holographic recording materials. Recently it has been shown that under influence of linear polarized light a lateral transfer of matter is possible allowing to realize “one step” surface patterning.

Already in 1976 Chomat *et al* [3] showed that a thin film of an amorphous  $\text{As}_2\text{Se}_3$  subjected to an intensity modulated red light interference pattern was significantly altered: a relief hologram was formed on the surface of the film. Almost twenty years later a similar phenomenon for thin layers of azo-benzene-containing polymers was observed by Rochon *et al* [4] and Kim *et al* [5]. A flat film can reach a corrugation whose amplitude may be up to fifty per cent of the initial thickness. It suggests that the material moieties are put in light-induced lateral transfer regarding the propagation direction of exciting light. The most commonly used method to induce mass motion is holographic recording with which a sinusoidal light intensity or polarization direction modulated pattern can

be obtained at the submicron scale. The surface relief structures can be formed also by a focused light spot [6] and illumination performed via a metal micro grid placed on the sample [7]. Recently, the surface relief grating recording only by one laser beam with lateral modulated polarisation directions was demonstrated [8]. The surface patterns can be erased by homogeneous illumination or heating above glass transition temperature of recording media. The SRG direct formation by two coherent laser beam interference has been observed in different disordered materials: in amorphous inorganic (As-S, As-Se) [3,7,9] and (Ge-Se) [10-12] chalcogenides, Sb-P-O oxide-containing glass [13] and organic (azo-benzene containing polymers [4,5,14], acrylamide photopolymers [15], carbazole-based azopolymer [16] and organic molecular glass [17] compounds.

The efficiency of SRG formation on the azobenzene containing polymer and chalcogenide semiconductor films strongly depends on the polarization state of the recording beams [9,18-20]. The largest surface relief (SR) modulation can be obtained under  $+45^\circ$ :- $45^\circ$  (linearly orthogonal polarization with a direction  $45^\circ$  regarding the plane of recording scheme) and RCP:LCP (right and left circular polarization of beams) recording conditions. It indicates that the existence of both light intensity gradient and resultant electric field variations is essential to the formation of SRG on amorphous chalcogenide and azobenzene polymer films.

A number of models have been proposed to explain the origin of the driving force responsible for SRG formation in the azo-polymers under the light illumination on the molecular level, including mean-field theory [21], permittivity gradient theory [22], gradient electric force

model [23] and other. There is still not general agreement on the origin of the driving force for this process and no mechanism yet proposed accounts for all experimental observations.

The main goal of this paper is to explore and compare the SRG formation efficiency in amorphous chalcogenides ( $\text{As}_2\text{S}_3$  and As-S-Se) and low molecular weight azobenzene containing organic glass films, as well as to establish the relationship between the SRG formation efficiency and photoinduced anisotropy in both materials.

## 2. Experimental

Thin films of amorphous  $\text{As}_2\text{S}_3$  and As-S-Se were prepared by thermal deposition on glass substrates at room temperature. The pressure during deposition was around  $10^{-6}$  Torr and the rate of deposition was  $\sim 20$  nm/s. The studied low molecular organic glass compound 4-((4-(bis(5,5,5-Triphenyl pentyl) amino) phenyl) diazenyl) benzoic acid (KRJ-8) was synthesized at Riga Technical University [24]. The molecular structure of the compound is shown in Fig. 1. The solution of KRJ-8 in  $\text{CHCl}_3$  was spin-coated on glass substrate. The thickness of dried films was determined by the Veeco Dektak 150 surface profilometer.

The surface relief (SR) formation experiments were performed using a holographic recording system described in [25]. The 491 nm, 532 nm, 561 nm and 594 nm laser orthogonally  $\pm 45^\circ$  linearly polarised light beams with equal intensity were used for holographic recording. Linearly polarised 653 nm laser beam at Bragg angle was used for read-out of diffraction efficiency. Diffraction efficiency ( $\eta$ ) was controlled in real time by measuring the 1st order diffracted beam intensity. The SRG recording efficiency was defined as the tangent of the slope angle  $\alpha$  of the linear increasing part of the diffraction efficiency (DE) curve [26]. The photo-induced surface relief of the films was measured by an atomic force microscope (AFM).

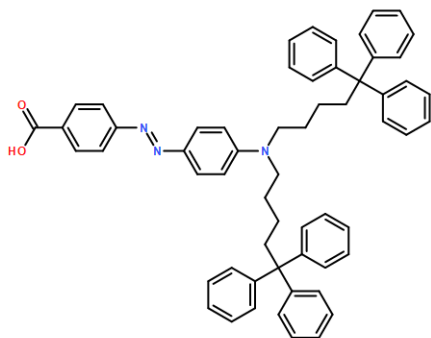


Fig. 1. Molecular structure of low molecular weight organic glass KRJ-8

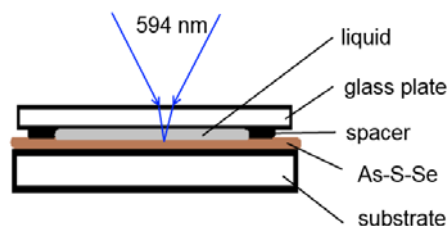


Fig. 2. A sample holder for the studies of influence of surface active liquids on SRG recording efficiency

Experimental set-up for photoinduced birefringence measurements is described in [25]. Birefringence was induced and measured by 532 nm laser light. A value of birefringence was evaluated according to formula:

$$\Delta n = \frac{\lambda}{\pi d} \arcsin \left( \sqrt{\frac{I}{I_0}} \right) \quad (1)$$

where  $I$  is the probe beam intensity passing through crossed polarizer and analyzer,  $I_0$  – probe beam intensity passing through parallel polarizers (with transmittance changes taken into account),  $\lambda$  - probe wavelength and  $d$  is the thickness of the studied film. A cell for the measurements of influence of surface tension of the studied chalcogenide films on the SRG inscription efficiency is shown in Fig. 2.

## 3. Results and discussion

Diffraction efficiency dependence on recording time in amorphous  $\text{As}_2\text{S}_3$  and KRJ-8 thin films is shown in Fig. 3a and Fig. 4a, respectively. Diffraction efficiency is directly correlated with the depth ( $\Delta h$ ) of the obtained relief (see Fig. 3b and Fig. 4b, respectively), thus to the efficiency of mass transport. Recording was performed until a saturation of diffraction efficiency and relief depth changes was reached. The recording curves of diffraction efficiency and SR changes can be expressed in three stages - nonlinear beginning (I), linear (II) and saturation (III) parts. To characterize the light sensitivity of the studied recording materials the slope of the linear part was calculated as a  $\tan \alpha$ . The values of  $\tan \alpha$  characterizing a recording rate of diffraction efficiency ( $V_\eta$ ,  $\% \cdot \text{cm}^2/\text{J}$ ) and SR depth ( $V_h$ ,  $\text{nm} \cdot \text{cm}^2/\text{J}$ ) for materials studied are shown in Table 1. There is a significant difference in light sensitivity of these two materials. The surface relief recording rate is  $7.4 \times 10^{-3}$   $\text{nm} \cdot \text{cm}^2/\text{J}$  and  $25$   $\text{nm} \cdot \text{cm}^2/\text{J}$  for  $\text{As}_2\text{S}_3$  and KRJ-8 films, respectively. It is known that one of the most important parameter of the materials used as a photoresist is a maximum value and its linear range of response to light illumination dose. For KRJ-8 films the linear range of surface relief changes is from recording starting up to 400 nm and the maximum changes are about 600 nm for grating period of  $1 \mu\text{m}$ . These parameters satisfy the main demands regarding the photoresist used for recording SR pixel holograms.

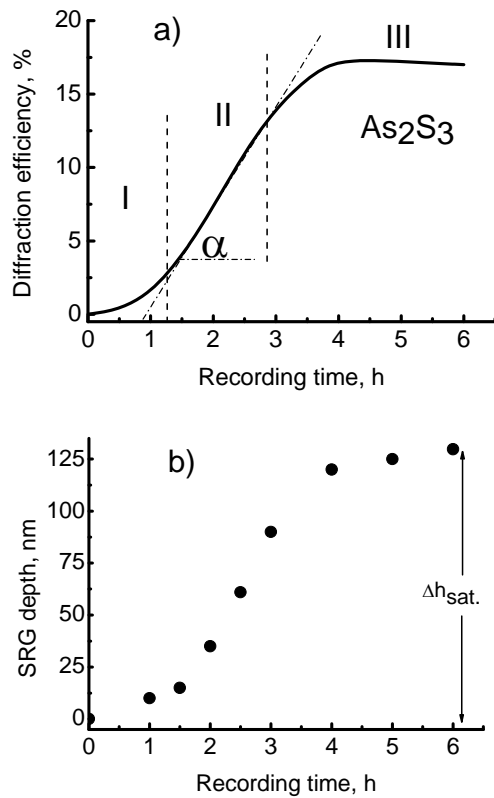


Fig. 3. Diffraction efficiency (a) and relief depth (b) of SRG recorded in 1.4 μm thick amorphous As<sub>2</sub>S<sub>3</sub> film. The orthogonally ±45° linearly polarised 532 nm laser light beams with intensity  $I_1=I_2=0.94$  W/cm<sup>2</sup> were used for holographic recording and s-linearly polarised 653 nm laser beam at Bragg angle for read-out of diffraction efficiency. Grating period  $\Lambda=1$  μm

The possibility of practical application of KRJ-8 films as a non-etching photoresist for production of embossed holographic labels is shown [24].

Analyzing the recording curves in Fig. 3 and Fig. 4, we can see a significant difference in the character of the initial stage (I) for As<sub>2</sub>S<sub>3</sub> and KRJ-8 films. The duration of this stage for As<sub>2</sub>S<sub>3</sub> films is about 1 hour, while the KRJ-8 films only take a few seconds.

The studies of initial stage (I) revealed the DE value and growth curve character dependence on the polarization state of read-out laser beam [26]. Fig. 5 and 6 illustrate the course of diffraction efficiency recording at s and p linearly polarized readout in As<sub>2</sub>S<sub>3</sub> and KRJ-8 films, respectively. The difference in the DE values between s- and p-polarized beam readout is observed. In the case of As<sub>2</sub>S<sub>3</sub> film the higher diffraction efficiencies are observed with s-polarized readout light, but for p-polarized readout light DE curve possesses a small maximum during first 200 seconds of recording. An opposite influence of read out light polarization direction is observed for KRJ-8 films. The higher DE values are observed for p-polarized readout and a small maximum is observed during first 10 seconds of recording beginning for s-polarized readout.

This phenomenon can be explained in the frame of polarization holography [27]. It is known that in chalcogenide [18,28,29] and azobenzene containing organic compound [27,30] thin films the photoinduced anisotropy can be observed. The interaction of an azobenzene-containing polymer with linearly polarized light results in an alignment of the dipole axis of the azo groups perpendicular to the polarization axis of the irradiated light, causing to birefringence and dichroism.

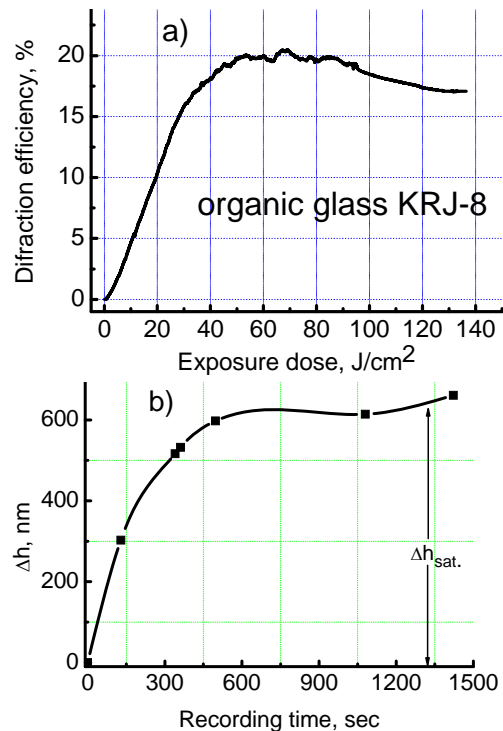


Fig. 4. Diffraction efficiency (a) and relief depth (b) of SRG recorded in 0.72 μm thick amorphous organic glass KRJ-8 film. The orthogonally ±45° linearly polarised 491 nm laser light beams with intensity  $I_1=I_2=50$  mW/cm<sup>2</sup> were used for holographic recording and s-linearly polarised 653 nm laser beam at Bragg angle for read-out of diffraction efficiency. Grating period  $\Lambda=1$  μm

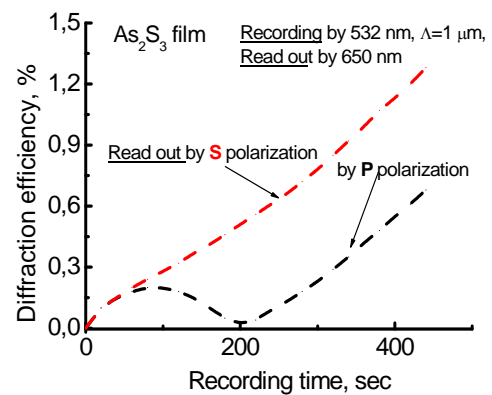


Fig. 5. Diffraction efficiency of SRG recorded in 5 μm thick amorphous As<sub>2</sub>S<sub>3</sub> film. The orthogonally ±45° linearly polarised 532 nm laser light beams with intensity  $I_1=I_2=0.94$  W/cm<sup>2</sup> were used for holographic recording and s- and p-linearly polarised 653 nm laser beams at Bragg angle for read-out of diffraction efficiency. Grating period  $\Lambda=1$  μm

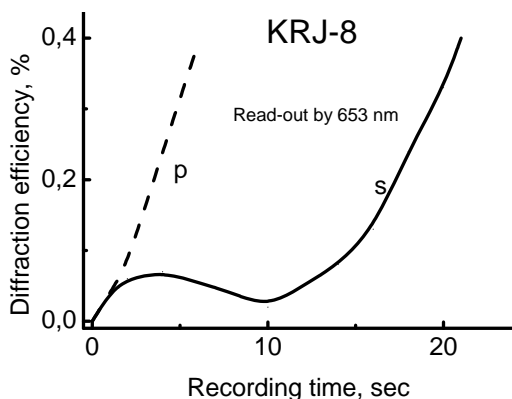


Fig. 6. Diffraction efficiency of SRG recorded in  $0.72 \mu\text{m}$  thick amorphous organic glass KRJ-8 film. The orthogonally  $\pm 45^\circ$  linearly polarised  $491 \text{ nm}$  laser light beams with intensity  $I_1=I_2=50 \text{ mW/cm}^2$  were used for holographic recording and  $s$ - and  $p$ -linearly polarised  $653 \text{ nm}$  laser beam at Bragg angle for read-out of diffraction efficiency. Grating period  $\Lambda=1 \mu\text{m}$

The photoinduced birefringence of KRJ-8 thin film is illustrated in Fig. 7. A high value of photoinduced birefringence ( $\Delta n \approx 0.2$ ) was obtained in this compound. The induction period of this birefringence value is very short in some seconds. Photoinduced birefringence in low molecular weight organic glass KRJ-8 (see molecular structure in Fig. 1) is mainly due to *trans*  $\leftrightarrow$  *cis* isomerization cycling of azo linkage ( $-\text{N}=\text{N}-$ ) when the chromophore absorbs a photon. Photoinduced molecular motions reduce the intra- and intermolecular interactions such as van der Waals force and hydrogen bonding by changing their interaction distances. The structure of KRJ-8 molecule is formed that azo linkage ( $-\text{N}=\text{N}-$ ) is surrounded by two triphenyl groups providing very low intermolecular interaction that can be characterized by very low surface tension  $\sigma=26.1 \text{ mN/m}$  [24]. Therefore electric field of linearly polarized light can easily orientate the molecule dipoles and the surface relief in the films of KRJ-8 compound is formed at relatively low exposure value indicating on a high mobility of the molecules under light influence.

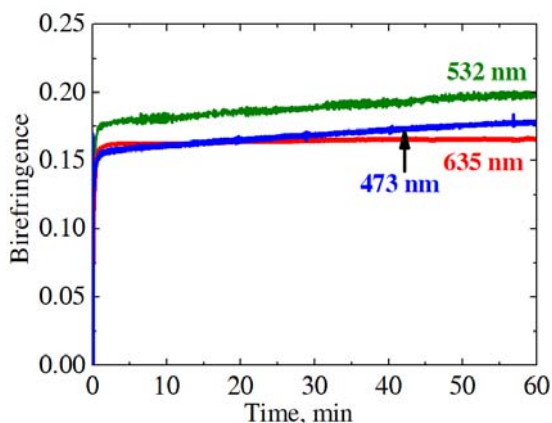


Fig. 7. Photoinduced birefringence in KRJ-8 induced by  $532 \text{ nm}$  laser ( $I=0.1 \text{ W/cm}^2$ ) and measured at  $473 \text{ nm}$ ,  $532 \text{ nm}$  and  $635 \text{ nm}$  light wavelengths

Induction period for photoinduced birefringence in amorphous  $\text{As}_2\text{S}_3$  films is much longer than for KRJ-8 films. According to [18,31] the induction period is measured in hours and a value of  $\Delta n$  is with order  $10^{-2} - 10^{-3}$ . Amorphous  $\text{As}_2\text{S}_3$  is an inorganic high molecular compound with network structure [29] and photoinduced anisotropy mainly can be arisen due to chemical bond breaking and switching. This process takes a lot of energy and long time. Therefore the induction period (I) for the SRG formation in  $\text{As}_2\text{S}_3$  films is more than 1 hour (see Fig. 3a).

It is known that the largest surface relief modulation can be obtained under  $+45^\circ$ :- $45^\circ$  (linearly orthogonal polarization with a direction  $45^\circ$  regarding the plane of recording scheme) and RCP:LCP (right and left circular polarization of beams) recording conditions [9,20,32]. For these configurations of recording beams there are components of resultant electric vector of light in interference pattern that are parallel and perpendicular to the grating vector direction [33] (Fig.8). The DE is determined by phase shift within one grating period. If optical path  $nd$  ( $d$ , thickness and  $n$ , refractive index of the film) in material illuminated by  $s$  and  $p$  polarized light differs, grating is formed and DE appears. Before irradiation there is no grating, thus  $n_s = n_p$ , where  $n_s$ , refractive index of ordinary ray and  $n_p$ , refractive index of extraordinary ray. When the recording process is started the photoinduced isomerisation and molecule alignment process takes place, and as a result photoinduced birefringence appears ( $n_s \neq n_p$ ) and volume polarization grating is formed. Before SR grating formation the DE both for  $s$  and  $p$  reading is equal. The result of this process is alignment of molecules perpendicularly to electric vector of the recording light (Fig. 8). When the formation of SRG has begun, the DE difference appears between the readings with  $s$  and  $p$  polarized light. For amorphous  $\text{As}_2\text{S}_3$  films the DE difference shows that volume polarization grating and SRG are in the phase or antiphase using the  $s$ -polarized or  $p$ -polarized readout light, respectively. In the case of the KRJ-8 film, the situation is the opposite. The coincidence of DE curves at the beginning of the SRG recording (Fig.5 and 6) for both  $s$ - and  $p$ -polarized measurements show that the initial process is due to the formation of volume polarization grating resulting from the formation and orientation of dipole moments during the holographic recording. The dipoles are able to acquire selective orientation reacting to the direction of the electric vector of the light according to interference pattern for  $+45^\circ$ :- $45^\circ$  configuration of holographic recording beams (see Fig. 8).

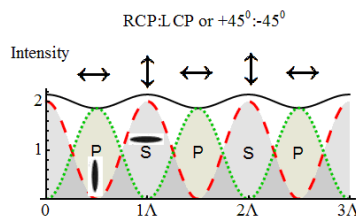


Fig. 8.  $s$ - and  $p$ - polarized light components in space-varying polarization pattern on sample for  $+45^\circ$ :- $45^\circ$  or LCP:RCP recording. An orientation of azo-dye molecules due to photoinduced anisotropy is shown for  $s$ - and  $p$ - components of light electric field

After the nonlinear initial phase (I), the linear phase (II) of the DE and SR depth increase is observed. For the KRJ-8 films, the linear stage (II) is started practically with holographic recording (Fig.4). It is due to the very fast stabilization of photoinduced birefringence value in this material (see Fig.7). The values of the recording rate of these two materials for the diffraction efficiency ( $V_{\eta}$ ,  $\% \cdot \text{cm}^2/\text{J}$ ) and SR depth ( $V_h$ ,  $\text{nm} \cdot \text{cm}^2/\text{J}$ ) are shown in Table 1. The surface relief recording rate is  $7.4 \cdot 10^{-3} \text{ nm} \cdot \text{cm}^2/\text{J}$  and  $25 \text{ nm} \cdot \text{cm}^2/\text{J}$  for  $\text{As}_2\text{S}_3$  and KRJ-8 films, respectively. So the SRG recording rate difference for both of these materials is about a thousand times.

The SRG recording in amorphous materials is influenced by many factors because the interaction between light and material strongly depends on both holographic recording conditions and properties of recording material. The relationship between molecular structure and photoinduced surface relief grating formation has been investigated by using azobenzene-based organic polymers and photochromic amorphous molecular materials [36]. The studies of molecular weight effect on the photoinduced surface relief gratings formation in a methacrylate azopolymer revealed that the grating inscription efficiency decreases with an increase of molecular weight [37]. The grating formation efficiency is clearly dependent on the length of the polymer chains in the material undergoing mass transport.

Low-molecular weight organic compound KRJ-8 in comparison with inorganic high molecular weight compound  $\text{As}_2\text{S}_3$  with network structure possesses lower glass transition temperature ( $T_g=107 \text{ }^\circ\text{C}$ ) and surface tension ( $\sigma=26.1 \text{ mN/m}$ ) facilitating the photoinduced mass displacement (see Table 1).

Table 1. Properties of amorphous  $\text{As}_2\text{S}_3$  and organic glass KRJ-8:  $T_g$  – glass transition temperature,  $^\circ\text{C}$ ;  $\sigma$  – surface tension,  $\text{mN/m}$ ;  $\Delta n$  – birefringence induced and measured at 532 nm

Material	$\text{As}_2\text{S}_3$	KRJ-8
Structure	Inorganic high molecular weight compound with network structure	Low-molecular weight organic compound
$V_{\eta}$ , $\% \cdot \text{cm}^2/\text{J}$	$\sim 10^{-3}$	0.55
$V_h$ , $\text{nm} \cdot \text{cm}^2/\text{J}$	$7.4 \cdot 10^{-3}$	25
$\Delta h_{\text{sat}}$ at $\Lambda=1 \mu\text{m}$	125 nm	>600 nm
Linear stage of SRG formation	20 -100 nm	0-400 nm
$T_g$ , $^\circ\text{C}$	200	107 [24]
$\sigma$ , $\text{mN/m}$	59 [34]	26.1 [24]
$\Delta n$	0.01	0.2

A number of proposed models for explaining the origin of the driving forces responsible for SRG formation under the light illumination on the molecular level, including mean-field theory [21], permittivity gradient theory [22], gradient electric force model [23], are based

on electromagnetic forces of the incident light. The spatial variation of the light (both intensity and polarization) leads to a variation of the material electrical susceptibility. The electric field of the incident light then leads to a polarization of the material. Forces are expected to occur between a polarized material and a light field gradient in a similar way as a dipole experiencing in an electric field gradient. According to [38] the presence of polar  $\text{As}_4\text{S}_3$  molecules which are sensitive to the electric field generated by the laser is responsible for observed laser-induced mass transport effect in amorphous As-S films.

To characterize the properties of polarized recording material the measurements of optical birefringence (see Fig. 7) and polarization holographic recording (Fig. 5 and 6) can be applied. From such point of view the effective formation of SRG in KRJ-8 films in comparison with chalcogenide material can be explained by high photoinduced birefringence ( $\Delta n=0.2$ ) of this material. The key role of photoinduced birefringence in the formation of SRG is confirmed by studies of  $\text{As}_4\text{S}_{6-x}\text{Se}_x$  films (see Table 2). The simultaneous increase of photoinduced birefringence and SRG depth is observed replacing sulfur by selenium.

The growth of the SRG becomes saturated at long inscription times (see Fig. 3 and 4). There is a large difference between saturation values of SRG depth ( $\Delta h_{\text{sat}}$ ) in  $\text{As}_2\text{S}_3$  and KRJ-8 films – 125 nm and >600 nm, respectively (see Table 1). According to [39] at large deformations the force of surface tension becomes comparable to the inscription force and therefore plays an essential role in the retardation of the inscription process. It is equal to zero when the surface is flat and increases proportionally to the surface area. The process of saturation depends on the counterbalance between the inscription force and the force of surface tension. This balance can be shifted in favour of the inscription force by a decrease of surface tension of recording medium. This can be realized by covering the recording film with the surface active liquid (see Fig. 2). The experiment was realized by SRG holographic inscription in  $\text{As}_{40}\text{S}_{15}\text{Se}_{45}$  films by 594 nm laser beams with a  $-45^\circ/+45^\circ$  configuration. The binary mixtures of water and isopropanol were used to obtain the liquids with a surface tension in the range of 21.7 – 35  $\text{mN/m}$  [40]. The obtained results are presented in Fig. 9. The SRG depth without covering liquid is of  $\Delta h_{\text{sat}}=200 \text{ nm}$ . An essential increase of  $\Delta h_{\text{sat}}$  values were obtained in the presence of covering liquids. It can be explained by a decrease of interphase surface tension between a chalcogenide film and a liquid thus promoting the SRG inscription process.

Table 2. Photoinduced birefringence ( $\Delta n$ ) and SRG depth ( $\Delta h$ ) in amorphous  $As_4S_{6-x}Se_x$  films; film thickness  $1 \mu m$ ; birefringence was induced ( $I_0=84 \text{ mW/cm}^2$ ) and measured at  $532 \text{ nm}$ ; SRG were recorded by  $532 \text{ nm}$  laser ( $I_1=I_2=0.6 \text{ W/cm}^2$ ) and exposure dose  $13.5 \text{ kJ/cm}^2$ ,  $A=1 \mu m$

Material	$As_4S_6$	$As_4S_5Se_1$	$As_4S_4Se_2$
Glass transition temperature ( $T_g$ ), $^{\circ}C$ [35]	200	197	194
$\Delta h$ , nm	73	155	177
$\Delta n$	0.010	0.015	0.018

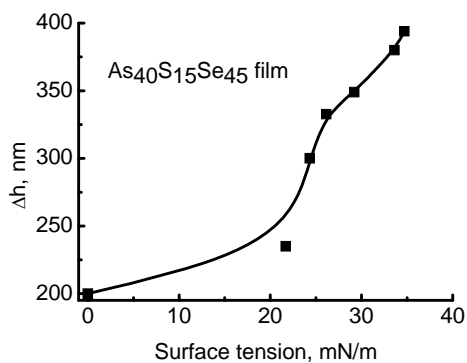


Fig. 9. Dependence of SRG formation efficiency in amorphous  $As_{40}S_{60-x}Se_x$  films on surface tension of covering liquid

#### 4. Conclusion

The direct holographic inscription of surface relief gratings (SRG) in amorphous chalcogenide and low molecular organic glass films induced by polarization direction modulated optical field was studied. The kinetic studies showed that the course of SRG growing curves can be divided in three development stages: an induction period of photoinduced birefringence, linear growing of SRG depth and saturation of SRG inscription process. The influence of the photoinduced birefringence on the relief formation process in amorphous chalcogenide ( $As-S$  and  $As-S-Se$  systems) films was evaluated and compared with the measurements on azo-benzene containing low molecular organic glass films. The best efficiency of surface relief grating (SRG) formation was observed with  $(+45^{\circ}, -45^{\circ})$  and (RCP, LCP) polarized beam combinations, which involve primarily variation in linearly polarized state across the film - parallel and perpendicular regarding the grating vector. It was shown that the saturation of SRG formation depends on the surface tension of recording material and a depth of SRGs can be enhanced by applying surface active substances to decrease the surface tension.

The SRG recording rate in  $As_2S_3$  and KRJ-8 films is  $7.4 \cdot 10^{-3} \text{ nm} \cdot \text{cm}^2/\text{J}$  and  $25 \text{ nm} \cdot \text{cm}^2/\text{J}$ , respectively. It means that in KRJ-8 films with an exposure dose about  $10 \text{ J/cm}^2$  is possible to obtain the SRG with a depth of  $250 \text{ nm}$  that is sufficient for application in holography.

#### Acknowledgements

Financial support by National research program IMIS2 is highly appreciated.

#### References

- [1] M. Kleman, O. D. Lavrentovich, *Soft Matter Physics: An Introduction*. Springer; 2003.
- [2] M. Popescu, A. Lorinczi, F. Sava, A. Velea, E. Matei, G. Socol, I. N. Mihailescu, *J. Optoelectron. Adv. M.* **10**, 2616 (2008).
- [3] H. Chomat, D. Ležal, I. Gregora, I. Srb, *J. Non-Cryst. Sol.* **20**, 427 (1976).
- [4] P. Rochon, E. Batalla, A. Natansohn, *Appl. Phys. Lett.* **66**, 136 (1995).
- [5] D. Y. Kim, L. Li, S. K. Tripathy, J. Kumar, *Appl. Phys. Lett.* **66**, 1166 (1995).
- [6] H. Hisakuni, K. Tanaka, *Appl. Phys. Lett.* **65**, 2925 (1994).
- [7] S. Kokenyesi, I. Ivan, V. Takats, J. Palinkas, S. Biri, I. A. Szabo, *J. Non-Cryst. Sol.* **353**, 1470 (2000).
- [8] E. Potanina, J. Teteris, *Chalc. Lett.* **10**, 449 (2013).
- [9] K. E. Asatryan, T. Galstian, R. Vallee, *Phys. Rev. Lett.* **94**, 08740 (2005).
- [10] I. Csarnovics, C. Cserhati, S. Kokenyesi, M. R. Latif, M. Mitkova, P. Nemeč, P. Hawlova, T. Nichol, M. Veres, *J. Optoelectron. Adv. M.* **18**, 793 (2016).
- [11] I. Csarnovics, M. Veres, P. Nemeč, M. R. Latif, P. Hawlova, S. Molnar, S. Kokenyesi, *J. Non-Cryst. Sol.* **459**, 51 (2017).
- [12] M. Reinfelde, M. Mitkova, T. Nichol, Z. G. Ivanova, J. Teteris, *Chalc. Lett.* **15**, 35 (2018).
- [13] F. S. De Vicente, M. Siu Li, Y. Messaddeq, *J. Non-Cryst. Sol.* **348**, 245 (2004).
- [14] B. Bellini, J. Ackermann, H. Klein, Ch. Graves, Ph. Dumas, V. Safarov, *J. Phys. Cond. Matter* **18**, S1817 (2006).
- [15] K. Pavani, I. Naydenova, S. Martin, V. Toal, *J. Opt. A: Pure Appl. Opt.* **9**, 43 (2007).
- [16] A. Meshalkin, S. Robu, E. Achimova, A. Prsacar, D. Shepel, V. Abaskin, G. Triduh, *J. Optoelectron. Adv. M.* **18**, 763 (2016).
- [17] H. Audorff, R. Walker, L. Kador, H. W. Schmidt, *Proc. SPIE* **7233**, 723300 (2009).
- [18] V. M. Kryshenik, M. L. Trunov, V. P. Ivanitsky, *J. Optoelectron. Adv. M.* **9**, 1949 (2007).
- [19] X. L. Jiang, L. Li, J. Kumar, D. Y. Kim, V. Shivshankar, S. K. Tripathy, *Appl. Phys. Lett.* **68**, 2618 (1996).
- [20] U. Gertners, J. Teteris, *Opt. Mat.* **32**, 807 (2010).
- [21] T. G. Pederson, P. M. Johansen, N. C. Holme, P. S. Ramanujam, *Phys. Rev. Lett.* **80**, 89 (1998).
- [22] K. G. Yager, C. J. Barret, *Current Opinion Sol. St. Mat. Sc.* **5**, 487 (2001).
- [23] J. Kumar, L. Li, X. Jiang, D. Kim, T. Lee, S. Tripathy, *Appl. Phys. Lett.* **72**, 2096 (1998).
- [24] A. Gerbreder, A. Bulanovs, J. Mikelsone, K. Traskovskis, E. Potanina, A. Vembris, J. Teteris, J.

- Non-Cryst. Sol. **421**, 48 (2015).
- [25] K. Klismeta, J. Teteris, IOP Conf. Series: MSE **77**, 012019 (2015).
- [26] J. Aleksejeva, M. Reinfelde, J. Teteris, Can. J. Phys. **92**, 842 (2014).
- [27] L. Nikolova, P. S. Ramanujam, Polarization holography. Cambridge University Press, 2009.
- [28] V. G. Zhdanov, V. K. Malinovskii, Sov. JTF Lett. **3**, 943 (1977).
- [29] K. Tanaka, K. Shimakava, Amorphous Chalcogenide Semiconductors and Related Materials, Springer, 2011.
- [30] T. Todorov, L. Nikolova, N. Tomova, Appl. Opt. **23**, 4309 (1984).
- [31] K. Tanaka, M. Notani, H. Hisakuni, Sol. St. Comm. **95**, 461 (1995).
- [32] U. Gertners, J. Teteris, J. Optoelectron. Adv. M. **11**, 1963 (2009).
- [33] J. Teteris, M. Reinfelde, J. Aleksejeva, U. Gertners, Physics Procedia **44**, 151 (2013).
- [34] A. T. Melnichenko, V. Fedelezh, T. Melnichenko, D. Sanditov, S. Badmaev, D. Damdinov, Glass Phys. Chem. **35**, 32 (2009).
- [35] J. S. Sanger, V. Q. Nguyen, I. D. Aggarwall, J. Am. Ceram. Soc. **79**, 1324 (1996).
- [36] H. Nakano, T. Tanino, T. Takahashi, H. Ando, Y. Shirota, J. Mat. Chem. **18**, 242 (2008).
- [37] C. J. Barrett, P. L. Rochon, A. L. Natansohn, J. Chem. Phys. **109**, 1505 (1996).
- [38] O. Kondrat, R. Holomb, A. Csik, V. Takats, M. Veres, V. Mitsa, Nanoscale Research Lett. **12**, 149 (2017).
- [39] M. Saphiannikova, T. M. Geue, O. Henneberg, K. Morawetz, U. Pietsch, J. Chem. Phys. **120**, 4039 (2004).
- [40] H. Ghahremani, A. Moradi, J. Abedini-Torghabeh, S. M. Hasani, Der Chemica Sinica **2**, 212 (2011).

---

\*Corresponding author: teteris@latnet.lv